Two-gluon exchange contribution to elastic $\gamma\gamma \to \gamma\gamma$ scattering and production of two-photons in ultraperipheral ultrarelativistic heavy ion and proton-proton collisions

Mariola Kłusek-Gawenda,[1,*] Wolfgang Schäfer,[1,†] and Antoni Szczurek[1,2,‡]

[1]*Institute of Nuclear Physics PAN, PL-31-342 Cracow, Poland*
[2] *University of Rzeszów, PL-35-959 Rzeszów, Poland*
(Dated: September 16, 2021)

Abstract

We discuss the two-gluon exchange contribution (formally three-loops) to elastic photon-photon scattering in the high-energy approximation. The elastic $\gamma\gamma \to \gamma\gamma$ amplitude is given in the impact-factor representation for all helicity configurations and finite quark masses. We discuss the importance of including the charm quark, which contribution, due to interference, can enhance the cross section considerably. We investigate the contribution to the $\gamma\gamma \to \gamma\gamma$ amplitude from the soft region, by studying its dependence on nonperturbative gluon mass. Helicity-flip contributions are shown to be much smaller than helicity-conserving ones. We identify region(s) of phase space where the two-gluon exchange contribution becomes important ingredient compared to box and nonperturbative VDM-Regge mechanisms considered in the literature. Consequences for the $AA \to AA\gamma\gamma$ reaction are discussed. Several differential distributions are shown. A feasibility study to observe the effect of two-gluon exchange is presented. We perform a similar analysis for the $pp \to pp\gamma\gamma$ reaction. Only by imposing severe cuts on $M_{\gamma\gamma}$ and a narrow window on photon transverse momenta the two gluon contribution becomes comparable to the box contribution but the corresponding cross section is rather small.

PACS numbers: 12.38.Bx, 25.75.Cj, 13.85.Qk

---

[*]Electronic address: mariola.klusek@ifj.edu.pl
[†]Electronic address: wolfgang.schafer@ifj.edu.pl
[‡]Electronic address: antoni.szczurek@ifj.edu.pl

I. INTRODUCTION

Recently a possibility of measuring elastic photon-photon scattering was discussed for the first time [1, 2]. Especially the recent calculation [2], which found a substantially larger cross section than earlier estimates, has rekindled the interest of LHC experiments. In this previous study of two of us [2], we have considered scattering via a fermion or W^+W^- loop (the so-called box mechanisms) as well as a nonperturbative mechanism of fluctuation of both photons into vector mesons and their subsequent interaction.

The second mechanism, which involves the Reggeon and Pomeron exchanges between vector mesons, leads to a rising elastic $\gamma\gamma$ cross section (see also [3] for the related $\rho^0\rho^0$ final state). Fermion boxes, due to the lower spin exchanged in the crossed channels, drop as a function of energy. The W^+W^--box, which gives a flat energy dependence becomes relevant only at large invariant masses of the diphoton system, $M_{\gamma\gamma} \gtrsim 2m_W$.

The hadronic Pomeron exchange contribution may dominate over the box mechanisms only at high subsystem energies, when the large contribution from the fermion boxes has died out, which means large rapidity distances between photons in heavy ion collisions.

Here we consider another mechansism which gives rise to a flat cross section at high $\gamma\gamma$ center of mass energy: the exchange of two gauge bosons between fermion-loops. In practice we restrict ourselves to the dominant two-gluon exchange contribution.

Formally the two-gluon exchange mechanism shown in Fig. 1 is a three-loop mechanism. Its contribution to the elastic scattering of photons at high energies has been first considered in the pioneering work [4]. Indeed in the limit where the Mandelstam variables of the $\gamma\gamma \to \gamma\gamma$ process satisfy $\hat{s} \gg -\hat{t}, -\hat{u}$, major simplifications occur and the three-loop process becomes tractable. This corresponds to a near-forward, small-angle, scattering of photons.

In our treatment, we go beyond the early work [4] by including finite fermion masses, as well as the full momentum structure in the loops, and we consider all helicity amplitudes.

The applicability of perturbative QCD (pQCD) requires a dominance of short distances, which should be ensured by a hard scale. As we deal with real photons, we are required to ask for a large momentum transfer, say $-\hat{t}, \ -\hat{u} \gg 1\,\mathrm{GeV}^2$.

The renewed interest to study $\gamma\gamma \to \gamma\gamma$ in heavy ion collsions makes the analysis of off-forward amplitude rather topical.

For reference we shall consider also the box mechansism (see left panel of Fig. 2) and the VDM-Regge mechanism (see right panel of Fig. 2.) where photons fluctuate into virtual vector mesons (three different light vector mesons are included). In this case the interaction "between photons" happens when both photons are in their hadronic states. The latter mechanism has very similar kinematics as the two-gluon mechanism discussed in the present paper in detail, but is concentrated at very small momentum transfers.
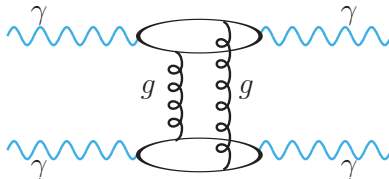

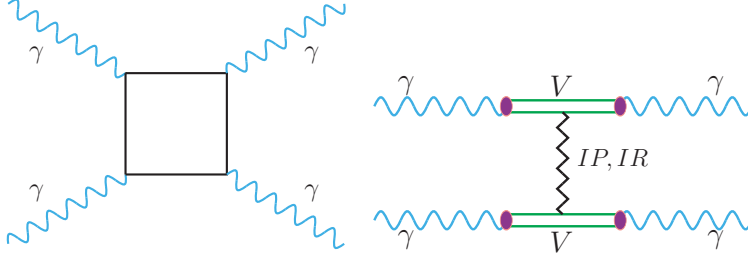FIG. 1: Elementary $\gamma\gamma \to \gamma\gamma$ processes via two-gluon exchange discussed in extenso in the present paper.

FIG. 2: Other elementary $\gamma\gamma \to \gamma\gamma$ processes. The left panel represents the box mechanism and the right panel is for VDM-Regge mechanism considered recently in Ref.[2].

II. THEORETICAL APPROACH

1. $\gamma\gamma \to \gamma\gamma$ elastic scattering

The altogether 16 diagrams of the type shown in Fig. 1 and Fig. 3 result in the amplitude, which can be cast into the impact-factor representation [5]:

$$\mathcal{M}(\gamma_{\lambda_1}\gamma_{\lambda_2} \to \gamma_{\lambda_3}\gamma_{\lambda_4}; \hat{s}, \hat{t}) = i\hat{s} \sum_{f,f'}^{n_f} \int d^2\boldsymbol{\kappa}\, \frac{\mathcal{J}^{(f)}(\gamma_{\lambda_1} \to \gamma_{\lambda_3}; \boldsymbol{\kappa}, \boldsymbol{q})\, \mathcal{J}^{(f')}(\gamma_{\lambda_2} \to \gamma_{\lambda_4}; -\boldsymbol{\kappa}, -\boldsymbol{q})}{[(\boldsymbol{\kappa} + \boldsymbol{q}/2)^2 + m_g^2][(\boldsymbol{\kappa} - \boldsymbol{q}/2)^2 + m_g^2]}\,. \tag{2.1}$$

Here $\boldsymbol{q}$ is the transverse momentum transfer, $\hat{t} \approx -\boldsymbol{q}^2$, and m_g is a gluon mass parameter, which role will be discussed below. We parametrize the loop momentum such that gluons carry transverse momenta $\boldsymbol{q}/2 \pm \boldsymbol{\kappa}$ (see Fig. 3). Notice, that the amplitude is finite at $m_g \to 0$, because the impact factors $\mathcal{J}$ vanish for $\boldsymbol{\kappa} \to \pm\boldsymbol{q}/2$.
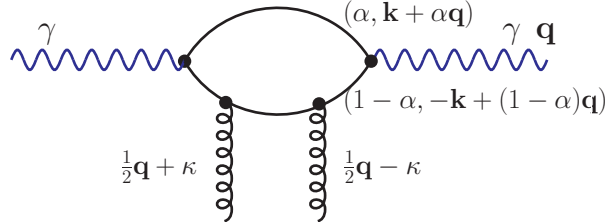

FIG. 3:   Kinematical variables used in calculating elementary $\gamma\gamma \to \gamma\gamma$ processes via two-gluon exchange.

The amplitude is normalized such, that the differential cross section is given by

$$\frac{d\sigma(\gamma\gamma \to \gamma\gamma; \hat{s})}{d\hat{t}} = \frac{1}{16\pi\hat{s}^2}\, \frac{1}{4} \sum_{\lambda_i} \left| \mathcal{M}(\gamma_{\lambda_1}\gamma_{\lambda_2} \to \gamma_{\lambda_3}\gamma_{\lambda_4}; \hat{s}, \hat{t}) \right|^2. \tag{2.2}$$

In this case, the explicit form of the impact factor is

$$\mathcal{J}^{(f)}(\gamma_\lambda \to \gamma_\tau; \boldsymbol{\kappa}, \boldsymbol{q}) = \sqrt{N_c^2 - 1} \; \frac{e_f^2 \alpha_{\text{em}}}{2\pi^2} \int_0^1 d\alpha \int \frac{d^2\boldsymbol{k}}{\boldsymbol{k}^2 + m_f^2} \alpha_S(\mu^2)$$

$$\times \left\{ \delta_{\lambda\tau} \left(m_f^2 \, \Phi_2 + \left[\alpha^2 + (1-\alpha)^2\right] (\boldsymbol{k}\Phi_1) \right) + \delta_{\lambda,-\tau} 2\alpha(1-\alpha) \left((\Phi_1 \boldsymbol{n})(\boldsymbol{k}\boldsymbol{n}) - [\Phi_1, \boldsymbol{n}][\boldsymbol{k}, \boldsymbol{n}] \right) \right\}.$$

$$(2.3)$$

Here, $\boldsymbol{n} = \boldsymbol{q}/|\boldsymbol{q}|$, and $[\boldsymbol{a}, \boldsymbol{b}] = a_x b_y - a_y b_x$. Furthermore, $N_c = 3$ is the number of colors, e_f is the charge of the quark of flavour f. Quark and antiquark share the large lightcone momentum of the incoming photon in fractions $\alpha, 1-\alpha$ respectively. The helicity conserving part is easily obtained, after due change of the final state wave function, from the one used in the $\gamma\gamma \to J/\psi J/\psi$ process in [6]. Also the helicity-flip piece can be obtained, mutatis mutandis, from the $\gamma \to V$ impact factors for vector meson final states [7].

Above Φ_1, Φ_2 are shorthand notations for the momentum structures, corresponding to the four relevant Feynman diagrams:

$$\Phi_2 = -\frac{1}{(\boldsymbol{l}+\boldsymbol{\kappa})^2 + m_f^2} - \frac{1}{(\boldsymbol{l}-\boldsymbol{\kappa})^2 + m_f^2} + \frac{1}{(\boldsymbol{l}+\boldsymbol{q}/2)^2 + m_f^2} + \frac{1}{(\boldsymbol{l}-\boldsymbol{q}/2)^2 + m_f^2},$$

$$\Phi_1 = -\frac{\boldsymbol{l}+\boldsymbol{\kappa}}{(\boldsymbol{l}+\boldsymbol{\kappa})^2 + m_f^2} - \frac{\boldsymbol{l}-\boldsymbol{\kappa}}{(\boldsymbol{l}-\boldsymbol{\kappa})^2 + m_f^2} + \frac{\boldsymbol{l}+\boldsymbol{q}/2}{(\boldsymbol{l}+\boldsymbol{q}/2)^2 + m_f^2} + \frac{\boldsymbol{l}-\boldsymbol{q}/2}{(\boldsymbol{l}-\boldsymbol{q}/2)^2 + m_f^2}, \quad (2.4)$$

and we have used

$$\boldsymbol{l} = \boldsymbol{k} + \left(\alpha - \frac{1}{2}\right)\boldsymbol{q}. \qquad (2.5)$$

In the present approach we assume incoming real photons and therefore only transverse photon polarizations are taken into account. This is a sufficiently good approximation for heavy-ion peripheral collisions where the nucleus charge form factor selects quasi-real photons.

The running scale of strong coupling constant for the evaluation of the two-gluon exchange cross section is taken as:

$$\mu^2 = \max\{\boldsymbol{\kappa}^2, \boldsymbol{k}^2 + m_Q^2, \boldsymbol{q}^2\}. \qquad (2.6)$$

We freeze the running coupling in the infrared at a value of $\alpha_S \sim 0.8$.

A. $AA \to AA\gamma\gamma$ reaction

As in our recent analysis [2] also here we follow the impact-parameter equivalent photon approximation [8], called in the following "b-space EPA" for brevity. In this approximation the cross section can be written as:

$$\sigma_{A_1 A_2 \to A_1 A_2 \gamma\gamma}(s_{A_1 A_2}) = \int d^2\boldsymbol{B} \, d^2\boldsymbol{b} \, \frac{d\omega_1}{\omega_1} \frac{d\omega_2}{\omega_2} \, \sigma_{\gamma\gamma\to\gamma\gamma}(\hat{s}) N\left(\omega_1, \boldsymbol{B} + \frac{\boldsymbol{b}}{2}\right) N\left(\omega_2, \boldsymbol{B} - \frac{\boldsymbol{b}}{2}\right) S_{abs}^2(\boldsymbol{b}).$$

$$(2.7)$$

4

Here $\hat{s} = M_{\gamma\gamma}^2 = 4\omega_1\omega_2$, and $N(\omega_i, \boldsymbol{b}_i)$ are the photon fluxes in one or second nucleus. Nuclear charge form factors are the main ingredients of the photon flux. In our calculations we use a realistic form factor which is a Fourier transform of a charge distribution in nuclei. More details about choice of the form factor and on derivation of Eq. (2.7) one can find in Ref.[9].

The gap survival factor, describing probability that the nucleus would not undergo break up, to a good approximation, can be written as ([2, 3, 8])

$$S_{abs}^2(\boldsymbol{b}) = \theta\left(|\boldsymbol{b}| - 2R_A)\right) . \tag{2.8}$$

Only some differential distributions can be calculated from formula (2.7). To make real comparison to future experimental data or made predictions for real experiments an inclusion of kinematical variables of individual photons is necessary. The corresponding details have been explained in Ref.[2] and will be not repeated here.

B. $pp \to pp\gamma\gamma$ reaction

In this paper we shall consider also the mechanism of elastic photon-photon scattering in $pp \to pp\gamma\gamma$ reaction. Here, in our exploratory study, we neglect the gap survival factor. Then the cross section of $\gamma\gamma$ production (via $\gamma\gamma$ fusion) in pp collisions takes the simple parton model form

$$\frac{d\sigma}{dy_1 dy_2 d^2 p_t} = \frac{1}{16\pi^2 \hat{s}^2} x_1 \gamma^{(el)}(x_1) x_2 \gamma^{(el)}(x_2) \overline{|\mathcal{M}_{\gamma\gamma \to \gamma\gamma}|^2} . \tag{2.9}$$

Here y_1, y_2 are the rapidities of final state photons, p_t is the photon transverse momentum, and

$$x_{1,2} = \frac{p_t}{\sqrt{s}} (\exp(\pm y_1) + \exp(\pm y_2)) . \tag{2.10}$$

In the numerical calculations for the elastic fluxes we shall use a practical parametrization of Ref. [10].

However, we should remember that for the proton-proton reaction another diffractive QCD mechanism takes place, the Pomeron-Pomeron fusion in which each Pomeron is treated as QCD ladder. As shown e.g. in [11] only at large invariant masses the $\gamma\gamma \to \gamma\gamma$ mechanism with intermediate boxes could win with the diffractive mechanism. Here we wish to analyze how the situation changes when the two-gluon exchange mechanism is taken into account.

III. NUMERICAL RESULTS

In our calculations here we take: $m_u, m_d = 0.15$ GeV, $m_s = 0.3$ GeV and $m_c = 1.5$ GeV. These are effective masses often used in dipole model calculations. These are parameters which allow to describe the cross section $\sigma_{\gamma p}$ even for quasi-real photons [12]. As far as m_g regularization parameter is considered we take two values: $m_g = 0.0, 0.75$ GeV. The first value is as for usual gluon exchange while the second one is suggested by lattice QCD [13] and the color-dipole analysis of high energy scattering, see e.g. [14] and references therein.

A. $\gamma\gamma \to \gamma\gamma$ **scattering**

In elastic $\gamma\gamma \to \gamma\gamma$ scattering all quark-loops contribute coherently in both impact factors (add up algebraically in the impact factors, which is squared then in the cross section). This means that adding only one flavour more changes the result considerably. This is particularly true for the charm quarks/antiquarks. The coherent effect is potentially large, much larger than for the total cross section where simple algebraic adding in each impact factor takes place.
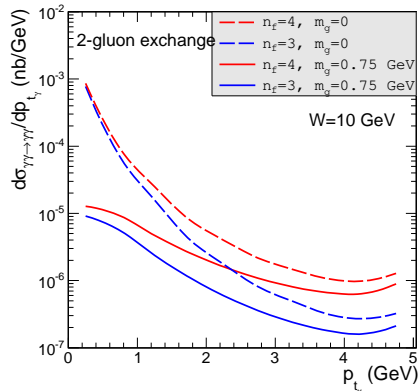
FIG. 4: Dependence on number of flavours included in the calculation of transverse momentum distribution of one of outgoing photons for the $\gamma\gamma \to \gamma\gamma$ elastic scattering. The result with three flavours is shown by the blue line, while that for four flavours by the red line.

In our calculation described above (Eq. (2.1)) n_f is left as a free parameter. Here we wish to discuss how our results depend on the number of flavours, n_f, included in the calculation. An example for $W = 10$ GeV is shown in Fig. 4. The results for three flavours are denoted by the blue lines and the results for four flavours by the red lines. In addition, we show distributions for vanishing and finite m_g. The figure shows that inclusion of four flavours is necessary. In general, the effect increases at larger transverse momenta.

The gluon mass has a large effect in a broad range of p_t, and very large p_t are necessary for convergence to the massless gluon pQCD limit ($m_g = 0$ - dashed lines, $m_g = 750$ MeV - solid lines). A similar observation was made in Ref. [15] for pion-pion elastic scattering.

Having fixed number of flavours we can focus on the role of the new mechanism. How important is the two-gluon contribution compared to the box and VDM-Regge contributions considered in [2] is illustrated in Fig. 5 for relatively low energy. Here the cross section differential in $z = \cos\theta$, where θ is the scattering angle in the $\gamma\gamma$ cms, is shown. The contribution of the VDM-Regge is concentrated at $z \approx \pm 1$. In contrast, the box contribution extends over a broad range of z. The two-gluon exchange contribution occupies intermediate regions of z. We need to add though, that the approximations made in the calculation of the two-gluon exchange are justified in a small angle region only. At small z the error can easily be 100%.

In Fig. 6 we show a difference between the case when s-channel-helicity is conserved (upper lines) and for helicity-flip piece (see Eq. (2.3)). The calculations show that the helicity-flip contributions are about three orders of magnitude smaller than the s-channel helicity conserving pieces. Note, that due to the zero mass of the photons, a helicity flip
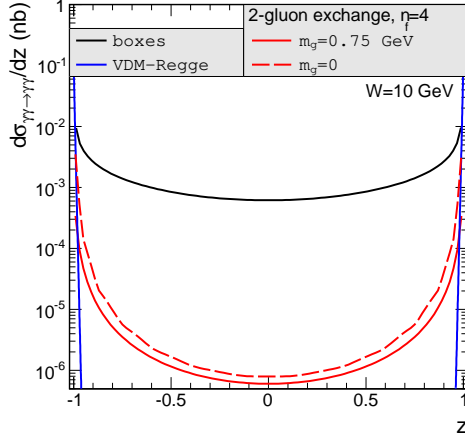
6

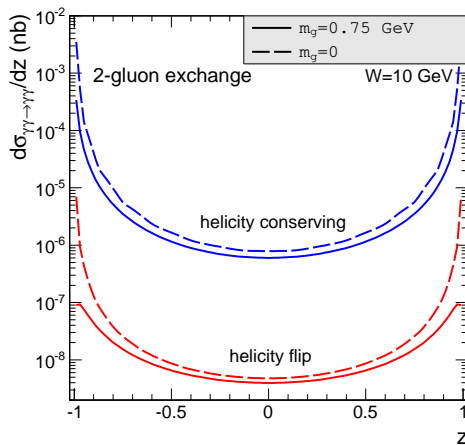FIG. 5: Competition of the three considered processes for $W = 10$ GeV.

FIG. 6: Comparison of helicity-conserving and helicity flip contributions for $W = 10$ GeV.

involves two units, the $\Delta\lambda = \pm 1$ processes which have some relevance in the vector meson production [7] are absent here.

Can the two-gluon exchange contribution be identified experimentally? To answer this question in Fig. 7 we show again the three contributions to transverse momentum distribution for quite different energies ($W = 10, 50, 200$ GeV). The soft VDM-Regge contribution occupies the region of very small transverse momenta, where it dominates. At low energies the two-gluon exchange contribution is always smaller than the VDM-Regge and box contributions. Increasing energy the situation improves for observing the influence of the two-gluon exchange mechanism. At $W = 50$ GeV there is a small window of photon transverse momenta 1 GeV $< p_t <$ 2 GeV where its contribution should be seen. At $W = 200$ GeV the window where the two-gluon is larger than the two other contributions extends now to 1 GeV $< p_t <$ 5 GeV. However, as was already pointed out in [4] (see also [16]) potentially a BFKL resummation of large logarithms $\log(\hat{s}/|\hat{t}|)$ could lead to a substantial enhancement of the $\gamma\gamma \to \gamma\gamma$ elastic scattering. This could be studied in a future. Clearly the effect could be studied experimentally in a future photon-photon collider (the photon-photon collider
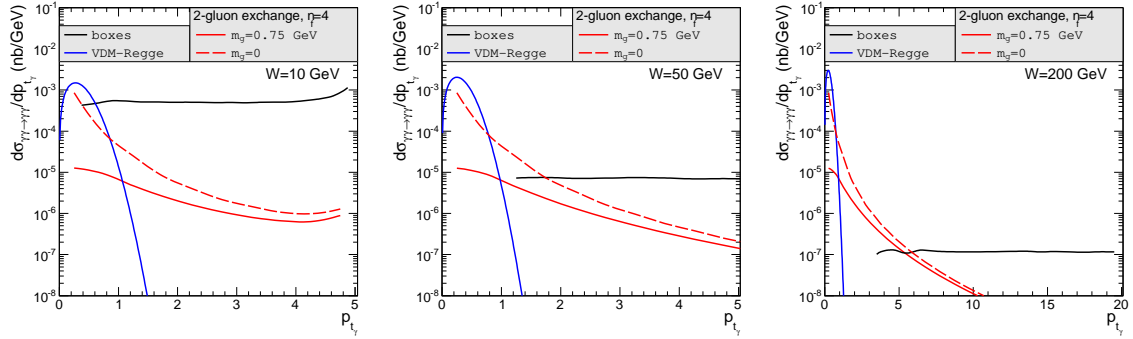
FIG. 7: Competition of different mechanisms for transverse momentum dependence of one of outgoing photons for the $\gamma\gamma \to \gamma\gamma$ elastic scattering. Individual contributions are shown separately.

could be realized at the facility of the International e^+e^- Linear Collider (ILC)). Now we wish to briefly investigate what could be the effect of the two-gluon exchange mechanism at the LHC both in ultraperipheral heavy-ion collisions and in exclusive $pp \to pp\gamma\gamma$ processes.

B. $AA \to AA\gamma\gamma$ process

In the near future ultrarelativistic collisions seems to be the best place to examine elastic photon-photon collisions [2]. In this case the cross section is enhanced by the $Z_1^2 Z_2^2$ factor compared to the proton-proton collisions, which for lead-lead collisions at the LHC ($Z_1 = Z_2 = 82$) is huge.

As in Ref.[2] we expect that the distributions in rapidity or rapidity difference between the two photons could be helpful in distinguishing the box and two-gluon exchange contribution. A lower cut on photon transverse momentum $p_t > 1$ GeV is necessary to get rid of the soft region where the VDM-Regge contribution dominates, as discussed in the previous subsection.

We see that the bigger distance between photons, the larger two-gluon to box contribution ratio is. Therefore we consider also a possibility to observe photons with forward calorimeters (FCALs). In Fig. 8 we show differential distribution as a function of $M_{\gamma\gamma}$ and $y_{diff} = y_1 - y_2$. The results are shown both for box and two-gluon exchange mechanisms. For comparison we also show contribution which comes from a $\gamma\gamma \to e^+e^-$ subprocess. We emphasise that this subprocess is a (reduceable) background to the light-by-light scattering.

In Fig. 9 we present $d\sigma/dy_1 dy_2$ map for boxes, two-gluon exchange mechanism (for $m_g = 0$ and $m_g = 0.75$ GeV) and for comparison a result for $PbPb \to PbPbe^+e^-$. We denote the coverage of the main detector ($-2.5 < y_{1/2} < 2.5$ - red square) and two smaller squares which represent situations when one photon is in one-side forward calorimeter and the second photon is in the second-side forward calorimeter.

C. $pp \to pp\gamma\gamma$ process

The $pp \to pp\gamma\gamma$ reaction is an alternative for the $AA \to AA\gamma\gamma$ studies. In the following we discuss first results for the $pp \to pp\gamma\gamma$ reaction. In Fig. 10 we show distribution in rapidity of one of the photons. The results are for different cuts on $M_{\gamma\gamma}$ and transverse momentum
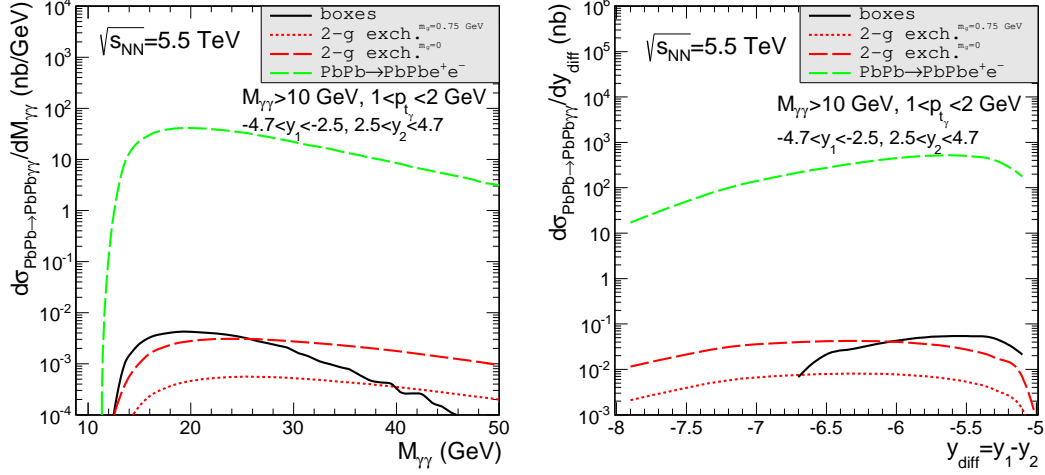
FIG. 8: Distribution in invariant mass of photons and in rapidity distance between the two photons for $M_{\gamma\gamma} > 10$ GeV, 1 GeV $< p_{t_\gamma} < 2$ GeV and $-4.7 < y_1 < -2.5$, $2.5 < y_2 < 4.7$. In addition, we show (top dashed, green line) a similar distribution for $AA \to AAe^+e^-$.
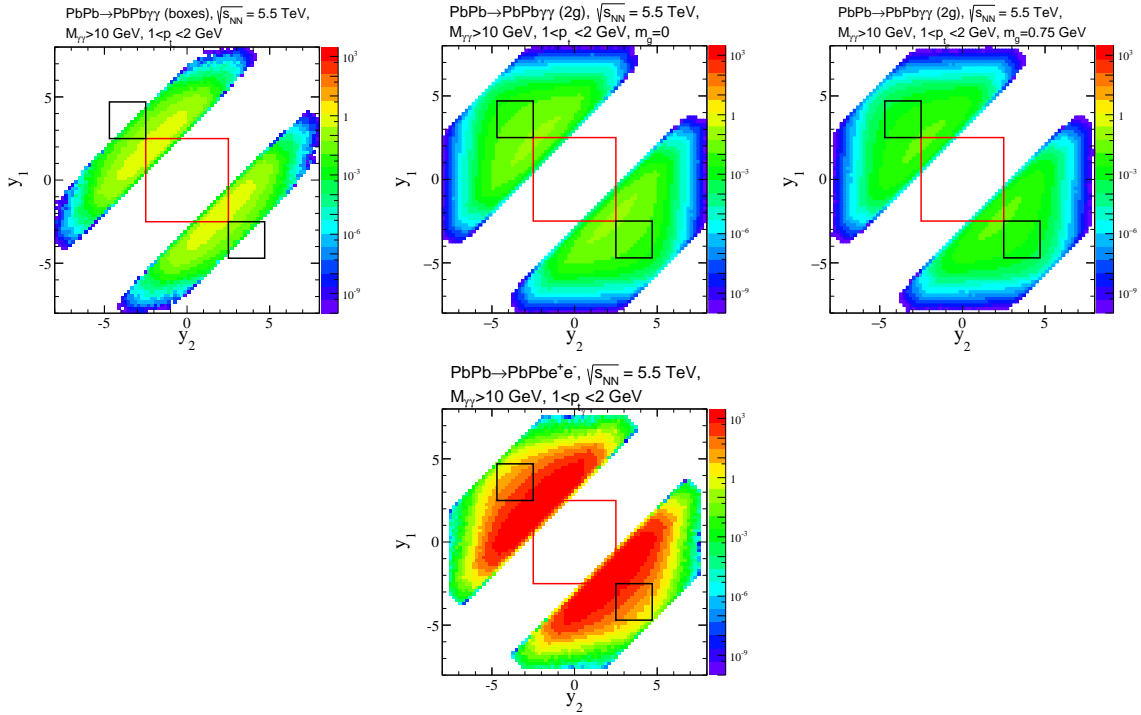

FIG. 9: Two-dimensional distributions in rapidities of the produced photons for the box mechanism, the two-gluon exchange mechanism and for the $AA \to AAe^+e^-$ process. Cuts on $M_{\gamma\gamma}$ and photon transverse momenta are specified in the figure legend.

of each of the photons. The results for two-gluon exchange contribution are shown with $m_g = 0$ (upper curve) and $m_g = 0.75$ GeV (lower curve). Even with the restrictive cuts, the two-gluon exchange contribution is less than 10 % of that for the boxes. The VDM-Regge

9

contribution is very small (negligible) as we have imposed lower cut on photon transverse momentum $p_t > 1$ GeV. As discussed in Ref.[2] the VDM-Regge contribution is very soft, concentrated dominantly for $p_t < 1$ GeV.
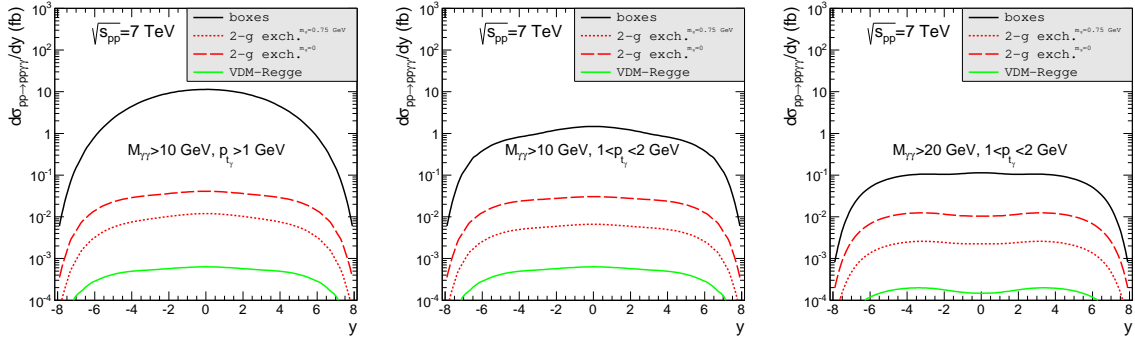

FIG. 10: Distribution in rapidity of one of the photons for different cuts specified in the figure legend.

The distribution in rapidity distance between both photons seems more promising (see Fig. 11). Increasing the lower cut on $M_{\gamma\gamma}$ and limiting to a narrow window in photon transverse momenta improves the relative amount of the two-gluon exchange contribution.
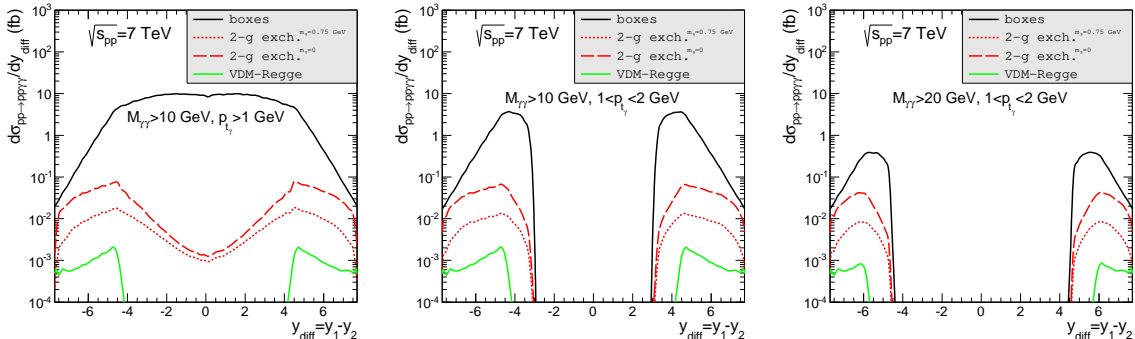

FIG. 11: Distribution in rapidity distance between the two photons for different cuts specified in the figure legend. No cuts on photon rapidities are applied here.

The distribution in the diphoton invariant mass is shown in Fig. 12. The two-gluon distribution starts to dominante over the box contribution only above $M_{\gamma\gamma} > 50$ GeV for 1 GeV $< p_t < 5$ GeV. However, the cross section in this region is rather small.

How the situation could change for larger collision energies is shown in Fig. 13 and Fig.14. The situation for the two presented distributions is rather similar for the LHC and Future Circular Collider (FCC)[1]. One advantage of larger collision energies are slightly larger cross sections. However, the dominance of the two-gluon exchange over the box contribution takes place more or less at the same diphoton invariant masses.

Below in Fig. 15 we show two-dimensional distributions in rapidities of photons produced in the $pp \rightarrow pp\gamma\gamma$ reaction. In this calculation we have assumed a cut on $M_{\gamma\gamma} > 10$ GeV

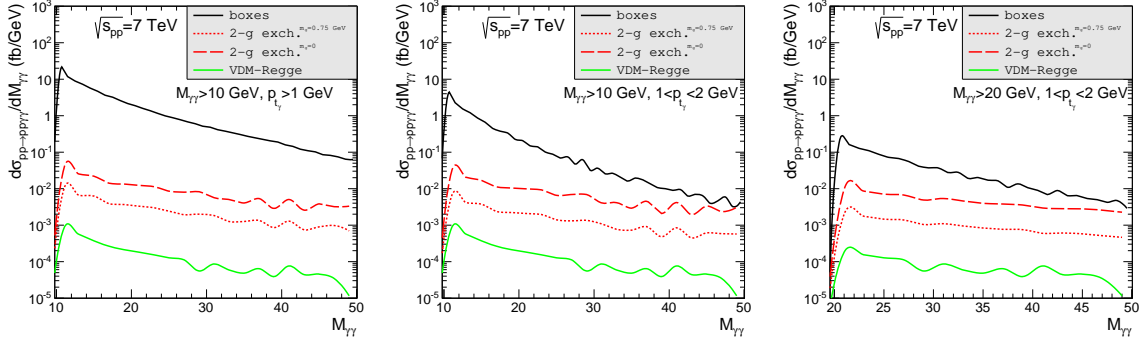[1] The box contribution to the pp, pA and AA cross sections at FCC was estimated in [17].

FIG. 12: Distribution in invariant mass of the produced photons for different cuts specified in the figure legend. No cuts on photon rapidities are applied here.
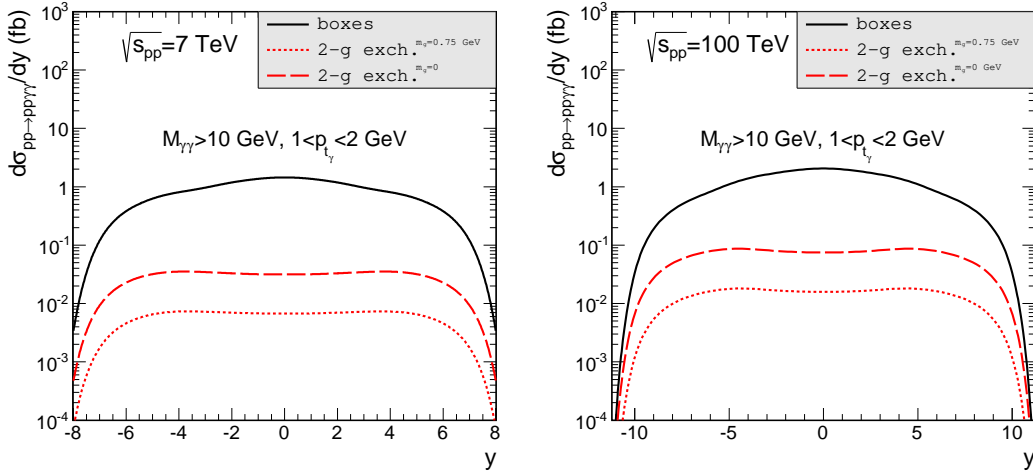

FIG. 13: Distribution in rapidity of the produced photons for $\sqrt{s} = 7$ TeV (LHC) and $\sqrt{s} = 100$ TeV (FCC) for cuts on photon transverse momenta specified in the figure legend. No cuts on photon rapidities are applied here.

and selected a narrow window on photon transverse momenta 1 GeV $< p_t <$ 2 GeV. The two-gluon exchange contribution starts to be larger only in very corner of the phase space when $|y_1 - y_2|$ is very large. We have marked the rapidity span of the main (CMS or ATLAS) detector (red central square) as well as for forward calorimeters (black smaller squares). It would be interesting to analyze whether the use of forward calorimeters could be possible in this context. Then the observation of one photon in one-side calorimeter and the second photon in the second-side calorimeter could help in observing the two-gluon exchange contribution. It is rather difficult to distinguish photons and electrons with the help of the calorimeters. At such a big rapidity distances ($5 < y_{diff} < 9.4$) the exclusive dielectron contribution [18] could be smaller.

Let us concentrate for a while on a measurement of photons with the help of forward calorimeters (ATLAS or CMS). To better illustrate the situation in Fig. 16 we show distributions in invariant mass of the two-photon system and in rapidity difference between one photon measured on one side and the second photon measured on the other side. The cross
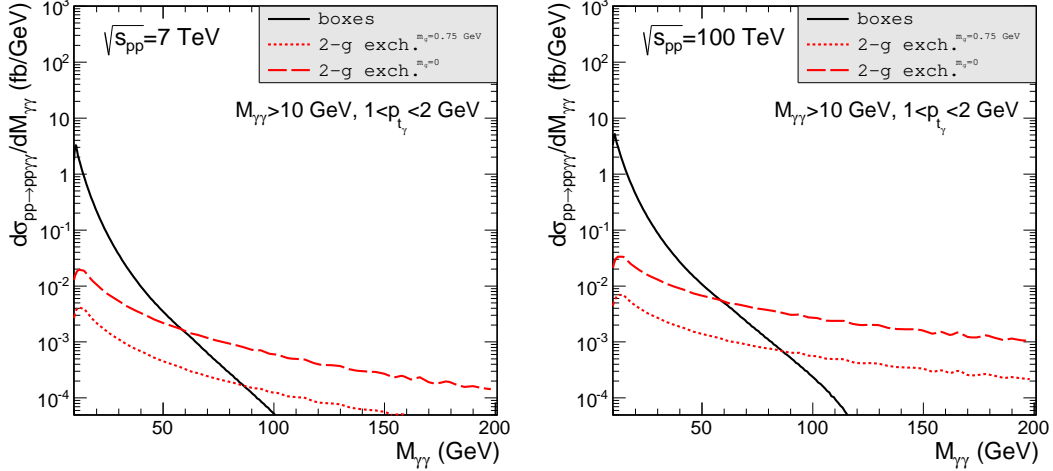
FIG. 14: Distribution in invariant mass of the produced photons for $\sqrt{s} = 7$ TeV (LHC) and $\sqrt{s} = 100$ TeV (FCC) for cuts on photon transverse momenta specified in the figure legend. No cuts on photon rapidities are applied here.
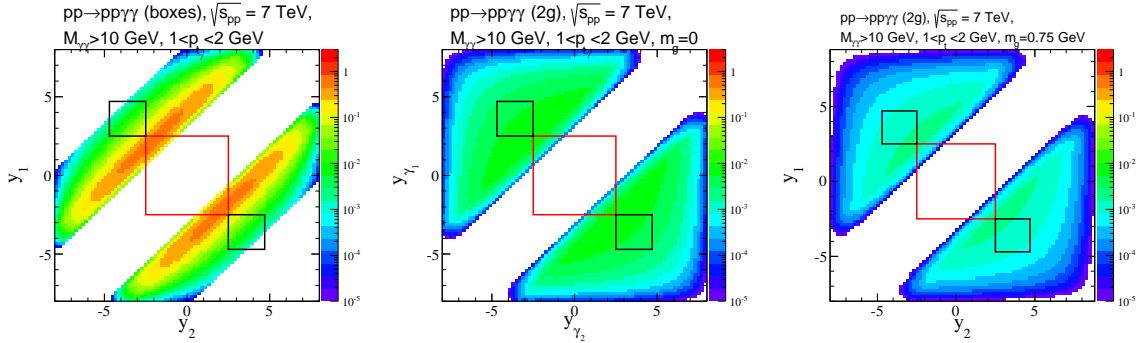

FIG. 15: Two-dimensional distributions in rapidities of the produced photons for the box mechanism and the two-gluon echange mechanism for cuts on $M_{\gamma\gamma}$ and photon transverse momenta specified in the figure legend. We show results both for $m_g = 0$ and $m_g = 0.75$ GeV.

section for the $pp \to pp\gamma\gamma$ process for the box contribution is larger than that for the two-gluon exchange up to $M_{\gamma\gamma} = 60$ GeV. For larger values of invariant mass of two photons the two-gluon exchange contribution (for $m_g = 0$) starts to dominate. For two-gluon exchange naturally the rapidity distances between the two photons are large. The two-gluon exchange contribution becomes larger for rapidity separations larger than seven or eight units. The corresponding cross sections are placed in Table 1. The two-gluon exchange contribution is only a small fraction of fb so the respective measurement would require large integrated luminosity which may be difficult in the light of pile-ups which are difficult to handle in the case of exclusive processes. Again the difference between two-gluon exchange contribution for massive ($m_g = 750$ MeV) and massless gluon exchange amounts to almost one order of magnitude.
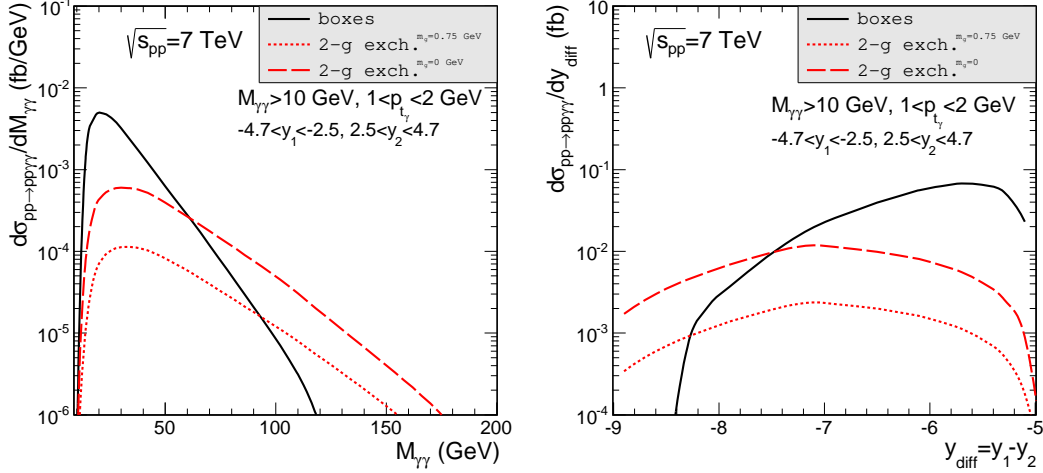
FIG. 16: Distributions in $M_{\gamma\gamma}$ (left panel) and in y_{diff} of the produced photons (right panel) for $\sqrt{s} = 7$ TeV (LHC). Here we assumed that one photon is measured in one-side calorimeter and the second photon in the second-side calorimeter. Other cuts are specified in the figure legend.

IV. CONCLUSIONS

Limitation	Mechanism	$\sigma_{PbPb \to PbPb\gamma\gamma}$ [nb]	$\sigma_{pp \to pp\gamma\gamma}$ [fb]
$M_{\gamma\gamma} > 10$ GeV,	boxes	7.307	12.524
1 GeV $< p_{t_\gamma} < 2$ GeV,	2g-exch. ($m_g = 0$)	1.234	0.317
$-8 < y_1 < 8$,	2g-exch. ($m_g = 0.75$ GeV)	0.260	0.067
$-8 < y_2 < 8$	$PbPb \to PbPbe^+e^-$	46 474.000	
$M_{\gamma\gamma} > 10$ GeV,	boxes	0.063	0.105
1 GeV $< p_{t_\gamma} < 2$ GeV,	2g-exch. ($m_g = 0$)	0.092	0.027
$-4.7 < y_1 < -2.5$,	2g-exch. ($m_g = 0.75$ GeV)	0.017	0.005
$2.5 < y_1 < 4.7$	$PbPb \to PbPbe^+e^-$	763.000	

TABLE I: Integrated cross section for the $\gamma\gamma$ production in lead-lead and proton-proton collisions for LHC energy $\sqrt{s_{NN}} = 5.5$ TeV and $\sqrt{s_{pp}} = 7$ TeV, respectively. We show results for $M_{\gamma\gamma} > 10$ GeV and 1 GeV $< p_{t_\gamma} < 2$ GeV for full range and for forward calorimeters. The nuclear cross section is calculated for ultraperipheral collisions of heavy ions.

In the present paper we have presented detailed formulae for the off-forward two-gluon exchange amplitude(s) for elastic photon-photon scattering, including massive quarks and all helicity configurations of photons. We have also performed first calculations of the corresponding component to the elastic photon-photon scattering. Both distribution in $z = \cos\theta$ and in transverse momentum of the outgoing photon have been presented. We have shown that helicity-flip contributions are extremely small compared to helicity-conserving ones. The two-gluon exchange component is rather small at small $W_{\gamma\gamma} < 20$ GeV compared to the well known box component. We have identified a window in photon transverse momentum (1 GeV $< p_t < 2$ GeV) where it may be, however, visible. At higher $W_{\gamma\gamma}$ energies the region where it wins becomes broader (1 GeV $< p_t < 5$ GeV). Furthermore the

cross section could be enhanced by potential BFKL resummation effects. This should be discussed in the future in more detail.

We have also made predictions for the $AA \to AA\gamma\gamma$ and $pp \to pp\gamma\gamma$ reactions including the previously neglected two-gluon exchange component. The calculation for ultraperipheral collisions have been done in the equivalent photon approximation in the impact parameter space, while the calculation for proton-proton collisions have been done as usually in the parton model with elastic photon distributions expressed in terms of proton electromagnetic form factors. In both cases we have tried to identify regions of the phase space where the two-gluon contribution should be enhanced relatively to the box contribution. The region of large rapidity difference between the two emitted photons and intermediate transverse momenta 1 GeV $< p_t <$ 2-5 GeV seems optimal in this respect.

However, the resulting cross sections are there rather small and huge statistics would be required to observe a sign of the two-gluon exchange contribution or its BFKL improvement (not yet available).

We have considered also an option to measure both photons by the forward calorimeters. It is rather difficult to distinguish photons from electrons in FCALs. In heavy-ion collisions, in addition, the cross section for $AA \to AAe^+e^-$ is huge, so this option seems not realistic. In $pp \to pp\gamma\gamma$ case the corresponding background would be smaller but the signal is also reduced.

[1] D. d'Enterria and G. G. da Silveira, Phys. Rev. Lett. **111** (2013) 080405 Erratum: [Phys. Rev. Lett. **116** (2016) 129901],

[2] M. Kłusek-Gawenda, P. Lebiedowicz and A. Szczurek, Phys. Rev. **C93** (2016) 044907,

[3] M. Kłusek, W. Schäfer and A. Szczurek, Phys. Lett. **B674** (2009) 92,

[4] I. F. Ginzburg, S. L. Panfil and V. G. Serbo, Nucl. Phys. **B284** (1987) 685,

[5] H. Cheng and T. T. Wu, Phys. Rev. **D1** (1970) 3414,

[6] S. Baranov, A. Cisek, M. Kłusek-Gawenda, W. Schäfer and A. Szczurek, Eur. Phys. J. **C73** (2013) 2335,

[7] I. P. Ivanov, N. N. Nikolaev and A. A. Savin, Phys. Part. Nucl. **37** (2006) 1,

[8] G. Baur and L. G. Ferreira Filho, Nucl. Phys. **A518** (1990) 786,

[9] M. Kłusek-Gawenda and A. Szczurek, Phys. Rev. **C82** (2010) 014904,

[10] M. Drees and D. Zeppenfeld, Phys. Rev. **D39** (1989) 2536,

[11] P. Lebiedowicz, R. Pasechnik and A. Szczurek, Nucl. Phys. **B881** (2014) 288,

[12] N. N. Nikolaev and B.G. Zakharov, Z. Phys. **C49** (1991) 607,

[13] E. Meggiolaro, Phys. Lett. **B451** (1999) 414,

[14] R. Fiore, N. N. Nikolaev and V. R. Zoller, JETP Lett. **99** (2014) 363,

[15] A. Szczurek, N. Nikolaev and J. Speth, Phys. Rev. **C66** (2002) 055206,

[16] N. G. Evanson and J. R. Forshaw, Phys. Rev. **D60** (1999) 034016,

[17] D. d'Enterria and G. G. da Silveira, arXiv: 1602.08088 [hep-ph],

[18] G. Kubasiak and A. Szczurek, Phys. Rev. **D84** (2011) 014005.